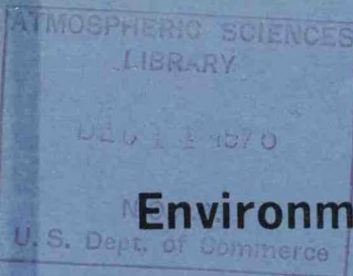


QC
880
.A4
no.
76/13



Environmental Research Laboratories
Air Resources
Atmospheric Turbulence and Diffusion Laboratory
Oak Ridge, Tennessee

June 1976

REGIONAL TRANSPORT MODEL OF ATMOSPHERIC SULFATES

K. S. Rao
I. Thomson
B. A. Egan

ATDL Contribution File No. 76/13

U. S. DEPARTMENT OF COMMERCE
NATIONAL OCEANIC AND ATMOSPHERIC ADMINISTRATION

QC
880
.A4
no. 76/13

REGIONAL TRANSPORT MODEL OF ATMOSPHERIC SULFATES

K. S. RAO

NOAA-ARL ATMOSPHERIC TURBULENCE &
DIFFUSION LABORATORY
OAK RIDGE, TENNESSEE

I. THOMSON AND B. A. EGAN

ENVIRONMENTAL RESEARCH & TECHNOLOGY
CONCORD, MASSACHUSETTS



LIBRARY
JUN 19 2015
National Oceanic &
Atmospheric Administration
U.S. Dept. of Commerce

**For Presentation at the 69th Annual Meeting of the
Air Pollution Control Association
Portland, Oregon June 27-July 1, 1976**

REGIONAL TRANSPORT MODEL OF ATMOSPHERIC SULFATES

K. S. Rao*, I. Thomson and B. A. Egan
Environmental Research & Technology, Concord, Mass. 01742

ABSTRACT

In recent years, there has been substantial evidence that particulate sulfate in the presence of sulfur oxide gases is a major contributor to the health hazards of air pollution, and there is considerable interest in developing a strategy for controlling the atmospheric sulfate concentration levels. This requires a systematic modeling program supported by observations aimed at understanding the relation between the emissions, chemical transformation, deposition, transport, and dispersion of sulfur oxides over distances of hundreds of kilometers from major sources.

As part of the Sulfate Regional Experiment (SURE) Design Project, a regional transport model of atmospheric sulfates has been developed. This quasi-Lagrangian three-dimensional grid numerical model uses a detailed SO_2 emission inventory of major anthropogenic sources in the eastern U.S. region, and observed meteorological data during an episode as inputs. The model accounts for advective transport and turbulent diffusion of the pollutants. The chemical transformation of SO_2 and SO_4^{m} and the deposition of the species at the earth's surface are assumed to be linear processes at specified constant rates.

The numerical model can predict the daily average concentrations of SO_2 and SO_4^{m} at all receptor locations in the grid region during the episode. Because of the spatial resolution of the grid, this model is particularly suited to investigate the effect of tall stacks in reducing the ambient concentration levels of sulfur pollutants. This paper presents the formulations and assumptions of the regional sulfate transport model. The model inputs and results are discussed. Isopleths of predicted SO_2 and SO_4^{m} concentrations are compared with the observed ground level values.

The bulk of the information in this paper is directed to air pollution meteorologists and environmental engineers interested in the atmospheric transport modeling studies of sulfur oxide pollutants.

INTRODUCTION

Recent experimental evidence suggests that particulate sulfates in the atmosphere contribute significantly to the health hazards of air pollution, adverse ecological effects due to increased acidity in lakes, corrosion and degradation of materials, and a general reduction in visibility. Current studies in the U.S. and Europe indicate that the exposure to sulfate particulates resulting from anthropogenic SO_2 emissions covers large regions extending for hundreds of kilometers downwind from major urban sources. Numerical model calculations supported by observations play an important role in understanding the relation between SO_2 emissions and atmospheric concentrations of SO_2 and SO_4^{m} .

A three-dimensional grid cell numerical model developed to investigate the regional transport of atmospheric sulfates is outlined in this paper. This model is an adaptation of the advection-diffusion transport model of Egan and Mahoney⁽¹⁾ based on a forward time explicit computational scheme which conserves not only the mass in each cell, but also certain statistical features of the mass distribution. The total mass in each grid cell is replaced by an equivalent rectangular pulse with the same mass, the same center of mass, and the same radius of gyration. This method suppresses the pseudo-diffusion errors that occur in the conventional finite difference procedures.

The numerical transport model essentially solves the mass conservation (tracer) equation which includes terms describing the horizontal advection transport, turbulent diffusion, emission, chemical transformation, and deposition processes.

Model Description and Formulations

This quasi-Lagrangian numerical model accounts not only for the advective transport in the horizontal by the mean wind, but the turbulent diffusion of the species as well. The masses are advected and dispersed each time step in the Lagrangian sense, and immediately afterwards a mass decomposition to the stationary Eulerian grid is performed. The horizontal emission grid has 26x17 cells covering a region of 2080 km (E-W) X 1360 km (N-S) in the eastern U.S. and southern Canada. To accomplish the turbulent diffusion calculations, the model has three air layers in the vertical, each of uniform depth over the grid region: 0-300m, 300-700m, 700-1500m. This allows the emissions to be introduced into one of the three layers depending on the effective effluent release height (stack height + plume rise) for elevated point sources. All ground-level point and area source emissions are introduced into the lowest layer next to the ground. Thus, this model is particularly suited to investigate the effects of tall stacks in reducing the atmospheric concentration levels of SO_x pollutants.

The mean wind field is assumed to be two-dimensional and the actual observed mean wind speeds (U and V components) at each horizontal grid cell are specified as model inputs at three or more vertical levels from the synoptic wind charts available at 12-hour intervals for the duration of the episode. For each time step, integration of the species conservation equations yields the instantaneous concentration distributions over the entire three-dimensional grid region consisting of 26x17x3 cells. The instantaneous concentrations in each cell are summed up and averaged over a 24-hour integration time period, to calculate the daily average concentrations which are then compared with the observed values at the receptor for that particular day. Thus, the three-dimensional numerical model can simultaneously predict the 24-hour average concentrations at all receptor locations in the grid region. The integration time period can be easily adjusted to be longer or shorter than 24 hours depending on the modeler's specific requirements.

The mass conservation equations of the pollutant species in a non-divergent flow field are given by:

$$\frac{\partial C_1}{\partial t} = -U \frac{\partial C_1}{\partial x} - V \frac{\partial C_1}{\partial y} + \frac{\partial}{\partial z} \left(K \frac{\partial C_1}{\partial z} \right) + \frac{Q}{h_1} - k_t C_1 \quad (1)$$

$$\frac{\partial C_2}{\partial t} = -U \frac{\partial C_2}{\partial x} - V \frac{\partial C_2}{\partial y} + \frac{\partial}{\partial z} \left(K \frac{\partial C_2}{\partial z} \right) + \frac{3}{2} k_t C_1 \quad (2)$$

where subscripts 1 and 2 denote SO_2 and SO_4^{\equiv} species respectively, C is the concentration, K is the vertical eddy diffusivity, Q is the SO_2 area-emission rate in the grid cell of height h_1 , and k_t is the transformation rate of SO_2 to SO_4^{\equiv} .

The deposition of the species at the earth's surface is described by the boundary condition:

$$\left[K \frac{\partial C}{\partial z} \right]_{z=0} = (1 - r) \bar{K} C_0 / \bar{h} \quad (3)$$

where r is a reflection coefficient defined by

$$r = 1 - V_d \bar{h} / \bar{K}, \quad 0 \leq r \leq 1 \quad (4)$$

In Eqs. (3) and (4), \bar{h} and \bar{K} are the mean depth and the mean eddy diffusivity of the lowest two vertical layers, C_0 is the ground-level concentration, and V_d is the deposition velocity of the pollutant. The latter is dependent upon the type of pollutant material, the type of deposition substrate, and the meteorological conditions. The measured deposition velocities for SO_2 generally range from 0.5 to 2.5 cm/s and for SO_4^{2-} from 0.1 to 0.5 cm/s⁽²⁾. By adopting representative values⁽³⁾ of $V_{d1} = 1$ cm/s and $V_{d2} = 0.1$ cm/s for the species, the deposition loss of material at the earth's surface can be simulated. The grid top boundary is assumed to be perfectly reflecting ($r=1$).

For wide area sources, the lateral spread of the plume by horizontal diffusion is negligible compared to the horizontal transport by mean wind and vertical turbulent diffusion⁽¹⁾. Therefore, the governing equations of the model do not include the horizontal diffusion terms.

Model Inputs

The total anthropogenic SO_2 emission rates (Q) are fixed by the emission inventory based on NEDS data, and specified in gms/m²/sec in each cell. The emissions are classified by the effective height of emission, season, and species, and stored on a computer disc for link-up with the computer program. A nominal wind speed of 5 m/sec is used in the plume rise calculations using Briggs' standard plume rise formula⁽⁴⁾ for near-neutral stability conditions.

For the duration of the episode, the observed mean wind speed and direction are available at each 1000 ft above the mean sea level at 12-hour intervals from the National Weather Service radiosonde data. The latter are plotted as U and V isotachs over the horizontal grid region of 26x17 cells for each vertical level and the winds are assigned numerical values at the center of each cell. These winds are corrected for the local topography and interpolated in the program to calculate the U and V components at the center of each vertical layer for each grid cell.

The model has the capability of incorporating temporally and spatially varying mixing depth (H) input data. In the present study, observed mixing depth data for the episode period modeled were not readily available, and a constant $H(x,y,t) = 1500m = \sum_{i=1}^3 h_i$ was assumed.

The K-profile specified as input to the model has the correct asymptotic behavior to simulate the diurnal and spatial variation of the eddy diffusivity. For simplicity, however, near-neutral stability conditions are assumed for the calculation of eddy diffusivity profile in this study from which discrete values of K are specified at the centers of the three vertical air layers.

Numerical Solution, Results and Discussion

The Egan-Mahoney numerical method, which conserves the zeroth, first, and second moments of mass distribution, is used to calculate the 5-D concentration of field SO_2 and SO_4^{2-} species from Eqs. (1) to (4). Details and discussion of this method can be found in References 1, 5 and 6.

The tracer equations are integrated with respect to time over a 24-hour period (October 5, 1974) selected for modeling. An integration time step $\Delta t = 1$ hour is determined such that it satisfies the criteria for convergence and stability of the numerical solution:

$$K_i \Delta t / h_i^2 \leq 0.5 \quad (5)$$

For each time step, the 3-D grid comprised of $26 \times 17 \times 3$ cells is swept twice to solve the two coupled tracer equations by calculating the three moments for each species. New wind inputs are specified every 12 hours. In spite of the complexity of the program, the computing times for a 24-hour integration are very reasonable (under five minutes) in the present study.

The calculated concentrations in level-1 are compared with the daily-average ground-level concentrations measured at ERT's AIRMAP[®] Network receptors for this sampling period. The available SO_4^- data from filter analyses are plotted against the predicted SO_4^- concentrations for two different values of the transformation rate as shown in Figure 1. The plot shows a good correlation between predictions and observations, and suggests a value of $k_t = 1$ to 2 percent per hour as appropriate for the model. A similar plot for the ground-level SO_2 concentrations is shown in Figure 2. Here also the agreement between observations and predictions is satisfactory. The comparatively small change between the predicted SO_2 concentrations for the two transformation rates indicates that the chemical sink term in Eq. (1) is not important.

For $k_t = 1$ percent per hour, the isopleths of the predicted daily average SO_4^- and SO_2 concentrations over the horizontal grid region in level-1 are shown in Figures 3 and 4, respectively. Similar isopleths for vertical levels 2 and 3 are shown in Figures 5 to 8. A qualitative comparison between the isopleths shows reasonable consistency with the emissions distributions. The ground level SO_2 distribution is strongly influenced by the surface and mid-level emissions localized over spatial scales of 0-100 km. The ground level SO_4^- distribution is more difficult to interpret in the light of the SO_2 emission inventory. The results suggest that the mid-level emissions strongly influence the estimated ground-level SO_4^- concentrations. It appears that intensive contributions to the latter occur from sources within an influence zone of 100-300 km, which justifies the regional scale model treatment of the atmospheric sulfate transport.

Conclusions

Numerical advection-diffusion models are useful tools to investigate the effect of meteorological conditions of air pollution interest on concentration distributions of sulfur pollutants in the atmosphere. Regional transport models, relating spatially and temporally varying SO_2 emissions to atmospheric SO_x concentrations are fundamental to the rational adoption of both short and long-term control strategies.

The results of the numerical model described in this paper suggest that advection of pollutants may be a dominant consideration on regional scale problems for slowly reactive pollutants. The Egan-Mahoney moment method was adopted primarily to reduce pseudo-diffusive errors in modeling advection. The model has the flexibility to incorporate variable inputs such as mean wind and turbulent diffusivity profiles and observed mixing depth data for sub-grid scale detail. Further, the chemical transformation and removal processes can be easily modeled as indicated in this paper.

The emphasis in this study was on adapting and developing the existing modeling tools to gain valuable insights into the regional transport of atmospheric sulfates. Viewed in this light, many of the simplifying assumptions of the model are justified. The satisfactory agreement between the calculated and observed concentrations is encouraging. However, more extensive observed concentration data are needed to fully calibrate and validate the model.

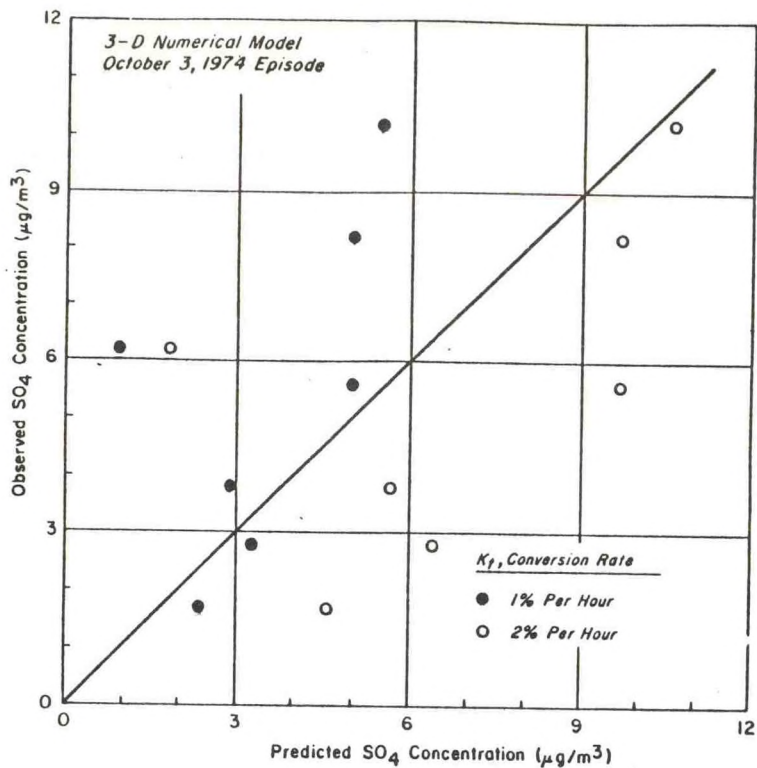
Acknowledgments

The work reported in this paper is part of the Sulfate Regional Experiment (SURE) Design Project sponsored by the Electric Power Research Institute (EPRI). The authors wish to acknowledge the assistance of Mrs. C. Ingersoll and Mr. D. McNaughton in the preparation of inputs to the model.

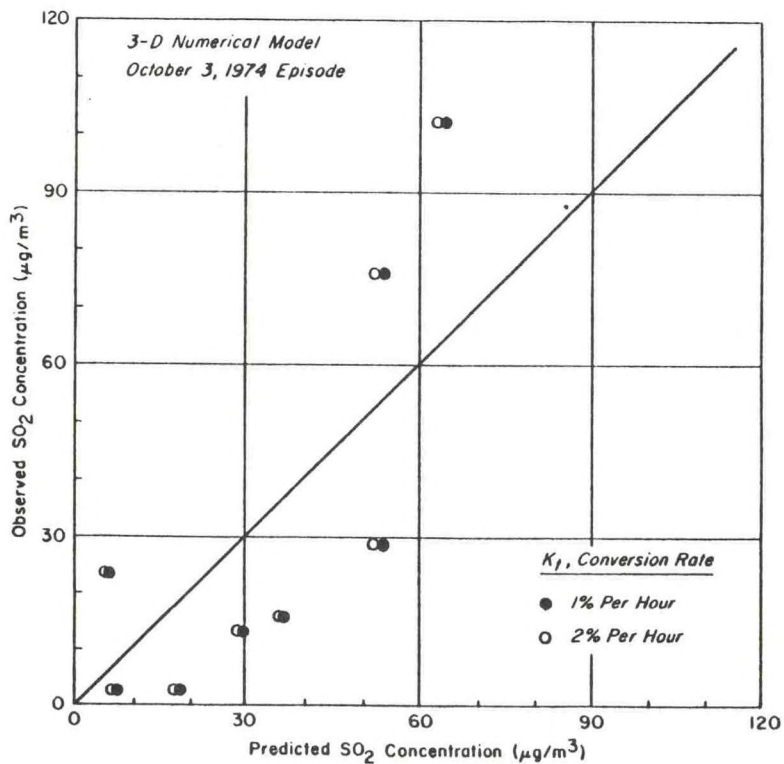
References

1. Egan, B.A. and J.R. Mahoney, Applications of a numerical air pollution transport model to dispersion in the atmospheric boundary layer, J. Appl. Meteorol., 11, pp.1023-1039, 1972.
2. SURE: Sulfate Regional Experiment Design Project. Report P-1586, Environmental Research & Technology, Inc., Concord, Mass. 01742, 1976, 500 pp.
3. Hidy, G.M., Removal processes of gaseous and particulate pollutants, Chap.III, Chemistry of the Lower Atmosphere, S.I. Rasool, ed., Plenum Press, New York, 1973, pp.121-173.
4. Briggs, G.A., Plume Rise, TID-25075, Clearinghouse for ESI, Springfield, Va. 22151, 1969, 82 pp.
5. Egan, B.A., and J. R. Mahoney, Numerical Modeling of Advection and Diffusion of Urban Area Source Pollutants, J. Appl. Meteor., 11, 312-322.
6. Pedersen, L.B. and L.P. Prahm, A method for numerical solution of the advection equation, Tellus, 26, No. 5, pp. 594-602, 1974.

*Present affiliation: NOAA-ARL Atmospheric Turbulence & Diffusion Laboratory, P. O. Box E, Oak Ridge, Tennessee 37830.



1. Comparison of predicted and observed ground level SO_4 concentrations.



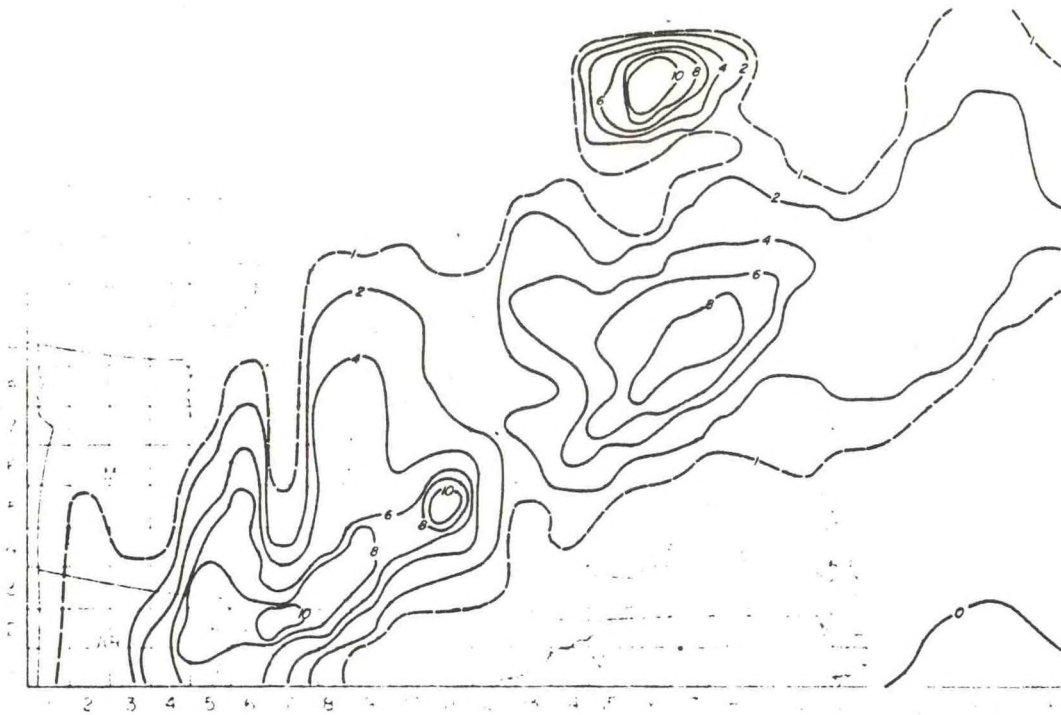
2. Comparison of predicted and observed ground level SO_2 concentrations.



3. Isopleths of calculated SO_4 concentrations ($\mu\text{g}/\text{m}^3$) in grid vertical level-1 for October 3, 1974.



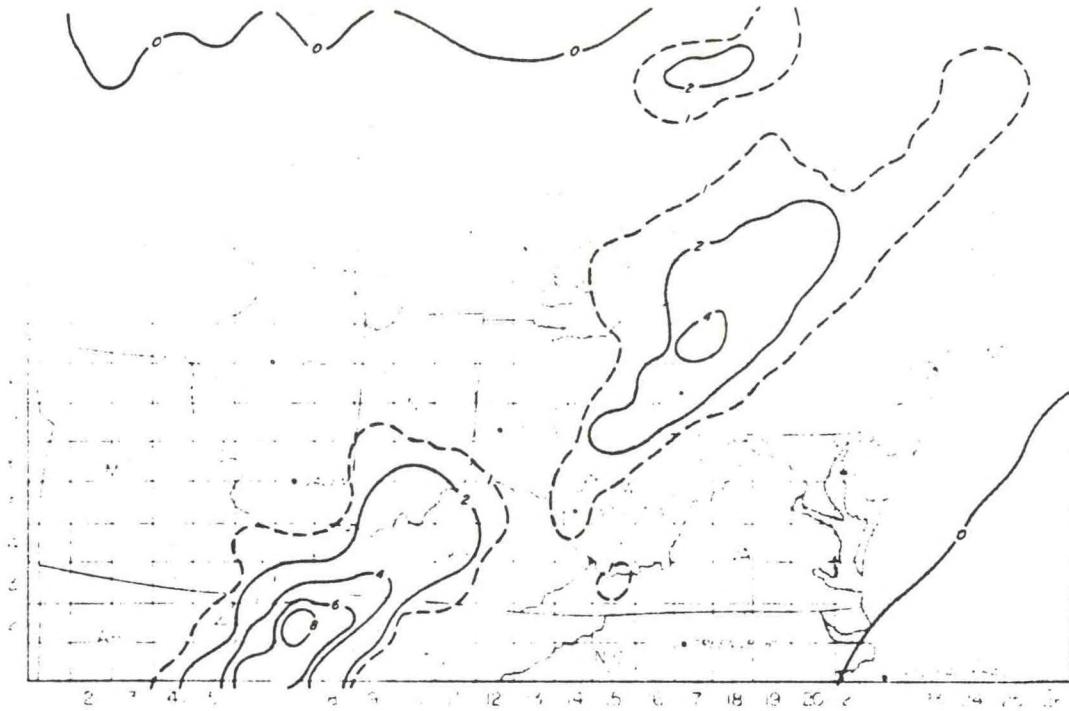
4. Isopleths of calculated SO_2 concentrations ($\mu\text{g}/\text{m}^3$) in grid vertical level-1 for October 3, 1974.



5. Isopleths of calculated SO_4 concentrations ($\mu\text{g}/\text{m}^3$) in grid vertical level-2 for October 3, 1974.



6. Isopleths of calculated SO_2 concentrations ($\mu\text{g}/\text{m}^3$) in grid vertical level-2 for October 3, 1974.



7. Isopleths of calculated SO_4^{2-} concentrations ($\mu\text{g}/\text{m}^3$) in grid vertical level-3 for October 3, 1974.



8. Isopleths of calculated SO_2 concentrations ($\mu\text{g}/\text{m}^3$) in grid vertical level-3 for October 3, 1974.